Radiant Ceiling Panels:

An Evaluation of Thermal Performance

Hung Q. Do [a], Mark B. Luther [b], Jane Matthews [a] (Corresponding author), Igor Martek [a], Peter Horan [a]

[a] School of Architecture and Built Environment, Deakin University, Geelong, VIC, Australia, 3220,

[b] Environmental Energy Services Pty. Ltd, Moolap VIC, Australia, 3224;

Email: qhdo@deakin.edu.au; mark.b.luther@gmail.com; jane.matthews@deakin.edu.au (Corresponding author); igor.martek@deakin.edu.au; peter.horan@deakin.edu.au

Abstract

Recently, many designs have been proposed for lightweight hydronic radiant ceiling panels, aiming at improving the panels' thermal performance and applications. However, the impacts of different panel designs on their performance, especially heat flux, surface temperature, and reaction time, require further investigation. Hence, this research proposes several designs for lightweight radiant ceiling panels with prototypes built. Instrumental experiments were conducted on the prototype panels, examining the aspects of their thermal performance, such as heat flux, surface temperature, response time, and thermal transmittance. By comparing the thermal performance of panels relatively, the effects of different designs on the thermal performance are revealed. The tribulations in the prototyping process were also used as an auxiliary aspect when comparing the panel designs. One design stands out to be thermally effective while being simple to produce. The testing results also show that the panels with lower thermal mass and better connection between the water tubes and the radiant surface yield higher thermal performance, including shorter response times, higher heat transfer, and better surface temperature. Also, the notable enhancement of cooling panel capacity caused by latent heat transfer is discussed.

Keywords: Thermal performance, cooling capacity, radiant panels, heat flux, time constant, heat transfer.

Highlight:

- Thermal connection and thermal mass are essential aspects of radiant panel design, significantly affecting the capacity of radiant cooling panels.
- Condensation risk can severely limit the capacity of radiant cooling but if condensation can be utilized, the capacity of radiant cooling panels can be enhanced notably.
- This study results in a design for radiant cooling panels that is practical, thermally effective, and mass produce ready.

1. Introduction

Radiant conditioning systems are known to be thermally effective and energy-efficient supplements to conventional convective air conditioning systems [1]. Instead of providing thermal comfort via air temperature control like their convective counterparts, radiant systems provide thermal comfort by controlling the Mean Radiant Temperature (MRT) [2]. This method of conditioning leads to several advantages over convective systems, such as reducing noise, draught risk, and local discomfort as well as being more energy efficient [2]. Hence, radiant systems have gained popularity among researchers, project owners, designers, and builders.

Usually, radiant systems are categorized into three types based on the configuration or design [3]. They are Radiant Panels (RP), Embedded Surface Systems (ESS), and Thermal Active Building Systems (TABS). It is well known that the configuration of radiant conditioning systems significantly impacts their thermal performance. For example, TABS are considered heavy radiant systems due to their high thermal mass, which leads to exceptionally long response times, increased energy use, difficulty with control, and thermal discomfort [2], making TABS unsuitable for dynamic thermal conditions such as perimeter zones in office buildings [4]. Also, TABS are difficult to install. Meanwhile, ESS and RP are

lightweight radiant systems with much faster response times and are easier to control [3] They can also be installed easily. Hence, such systems are gaining popularity [5].

Previous research has demonstrated that the thermal mass and the thermal connection between the capillary tubes and the radiant surface can significantly impact the panels' conditioning capacity, and reaction time [6]. Building on this previous research, we aim to provide a deeper understanding of the impacts of panel design, thermal mass, and thermal connection on the panels' performance. Also, this study aims to advance radiant cooling panel design by improving construction methods and overall performance. Six panel designs are proposed focusing on enhancing thermal performance while maintaining ease of construction. Panel prototypes are built for the six designs, and their thermal performance is tested and evaluated.

2. Radiant Panel Design

All six new designs used the same "canopy to canopy" capillary tube mat. The "canopy to canopy" piping and water distributing model is recommended by Mosa, Labat [7] for radiant systems. It can evenly distribute water, reduce flow resistance, and shorten flow distance, leading to higher performance for radiant systems. 25mm thick rigid insulation boards are used as the primary insulation layer on the back of the panels. This insulation board is lightweight, sturdy, and has a high R-value of 1.05 m^2K/W. Details of the designs are shown in Fig. 1.

In Design 1, the capillary tubes are embedded inside the ceiling tile. The prototype of this design (P1 routed) is about 6kg. This design proved to be thermally effective, yielding high heat flux output and fast response due to its high thermal connection between the capillary tubes and the radiant surface [6]. However, the prototyping process of this design is also complicated and costly. Trenches must be routed using sophisticated machinery to embed the capillary tube inside the gypsum ceiling tile. Also, this machining produces a large amount of dust and waste.

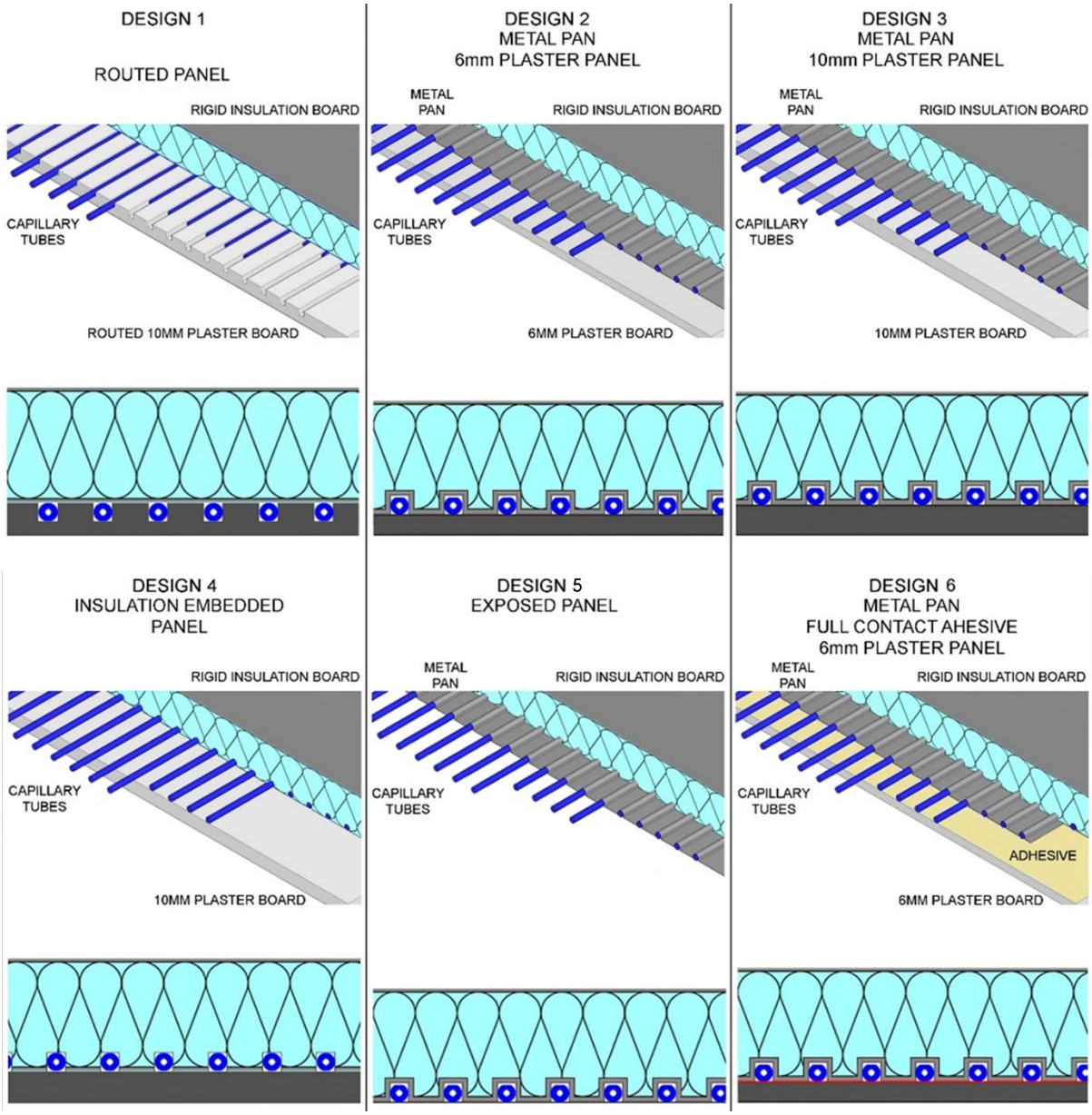

Fig. 1. Panel designs

Designs 2 and 3 are similar to each other. These designs are based on 'Type B' of the Embedded Surface Systems (ESS) according to the REHVA handbook for radiant systems [3]. The capillary tubes are embedded in the insulation layer rather than inside the radiant surface, a 6 mm thick gypsum ceiling tile for Design 2 and 10mm for Design 3. Thus, the only difference between the two designs is the thermal mass of the radiant surface. To increase the thermal connection and conduction between the capillary tubes and the radiant surface, metal pans (aluminum) are added. The pans are 0.3mm thick and shaped

so that they wrap around the capillary tubes. Design 2 (P2 Pan + Plaster 6mm) weighs 5kg, while Design 3 (P3 Pan + Plaster 10mm) is 6.5kg.

Design 4 is a simplified version of Design 3. Design 4 has no heat transfer pan, and the capillary tubes are embedded directly into the insulation layer. The radiant surface is a 10mm thick gypsum ceiling tile. Hence, this can also be considered a version of the 'Type B' ESS. This design is simple to prototype, with the panel (P4 Insulation Embedded) weighing about 6.5kg.

Design 5 exposes the tubes and heat transfer pans; no radiant (finish) surface is added. This panel demonstrates the impact of having no thermal mass or thermal resistance (R-value = 0) added by the finishing surface. The panel (P5 Exposed) weighs just 1 kg and does not contain gypsum ceiling tile.

Design 6 is an improved version of Design 2. Instead of having the pans and tubes "touch" the ceiling tile, adhesive (glue) is applied to connect the pipes and pans with the radiant surface. This adhesion method allows the components of the panel to have thermal "full contact" with each other, thus enhancing heat transfer. This panel (P6 Full Contact) also weighs 5kg.

A prototype is constructed for each panel design. The prototyping process shows that the panels can be built with relative ease. Even the aluminum heat transfer pans can be easily made with a jig and basic hand tools.

3. Research Approach

This section describes the process of testing, measuring, and evaluating the performance of the panel prototypes and analyzing the data. In this study, empirical experiments are rigorously conducted with instrumental measurements recorded, and the performance of the panel prototypes is evaluated by way of related quantitative parameters. The panels are evaluated according to their relative thermal performance and the panels' design and prototyping process.

3.1. Research Method and Design

Three test runs were conducted; each consisted of 4 panels and focused on investigating a particular attribute, and the panels were selected accordingly. Test 1 focuses on the impact of thermal connection on the panels' energy output (heat flux). Here, the panels are chosen to provide a variety of thermal connection configurations: embedded connection for Design 1, metal pans connection for Design 2 and 3, and "touch" connection for Design 4.

Test 2 investigates the effect of thermal mass and thermal resistance of the radiant surface (the gypsum board ceiling tile). Hence, the panel of Design 4 (P4 Insulation Embedded) is replaced by Design 5 (P5 Exposed). Here, the panel of Design 5 (P5 Exposed) has no gypsum board ceiling tile (no added thermal mass nor thermal resistance), allowing it to perform at a higher potential. Hence, it can be used as a benchmark to analyze the performance of other panels. Meanwhile, the Design 1, 2, and 3 panels have different radiant surface configurations.

Test 3 was the final test run using the lessons learned from the abovementioned tests. The panel of Design 6 (P6 Full Contact) was introduced, replacing that of Design 5 (P5 Exposed). Design 6 is expected to be the "go-to" design, overcoming the shortcomings of the others. Hence, Test 3 compares the performance of the Design 6 panel (P6 Full Contact) with Design 1, 2, and 3, so that the effect of enhanced thermal connection and low thermal mass can be revealed.

Fig. 2 below shows the test runs and the panel designs with their properties. The parameters being evaluated in the experiments are also indicated. The test runs are designed to highlight the importance of thermal connection, thermal resistance, thermal mass, and the overall design in terms of composition.

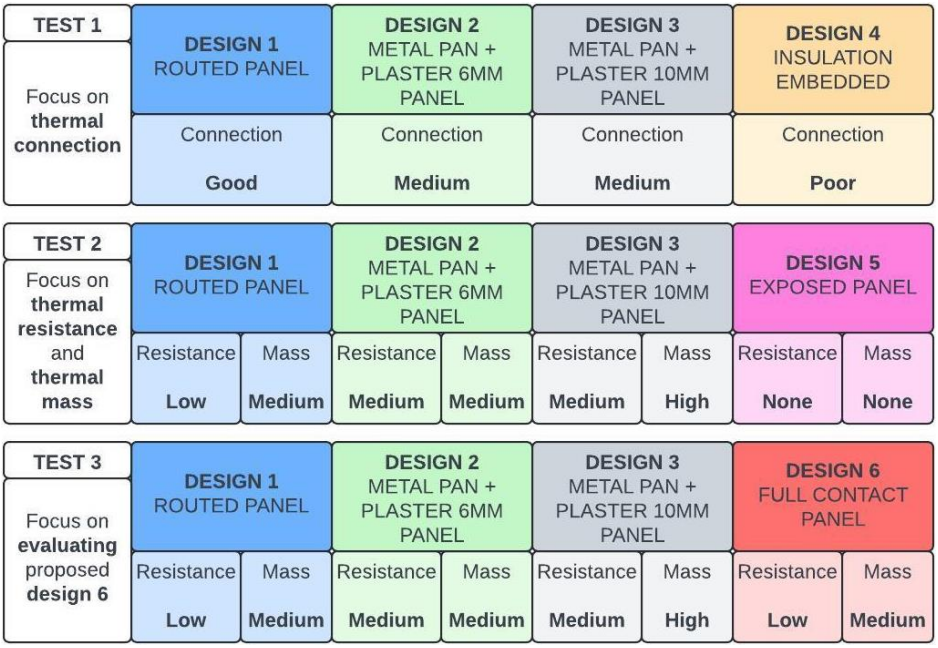

Fig. 2. Test runs and subject panel designs with their expected property

3.2. Variable to be Measured and Calculated

Table 1 shows the parameters to be assessed in this study. Overall, to evaluate radiant panel performance four variables are directly measured, including the radiant surface temperature (T_s), water temperature inside the panel (T_w), the total heat flux (q), and the ambient operative temperature (OT_i). Additionally, a mathematical model can calculate the time constant (TC). The water flow rate is also measured to verify the operation of the radiant system.

Table 1

Variables to be measured and calculated

Variable	Symbols	Unit	Collection
Radiant surface temperature	T_s	°C or K	Thermocouple
Heat flux (heat transfer)	q	W/m²	Heat flux sensor
Heat transfer coefficient	H_t	W/m²K	Calculation
Time constant	TC	Minute	Calculation
Air velocity	v	m/s	Thermal comfort cart
Operative temperature	OT_a	°C or K	Calculation
Inlet water temperature	T_w	°C or K	Thermocouple
Water flowrate	f	L/min	Flowmeter

3.3. Direct Measurement and Calculation.

Fig. 3 illustrates a measurement for the panel of Design 1 (P1 routed) in an auxiliary test run. Here, the radiant surface temperature (T_s), water temperature inside the panel (T_w), total heat flux (q), and ambient operative temperature (OT_a) are measured directly.

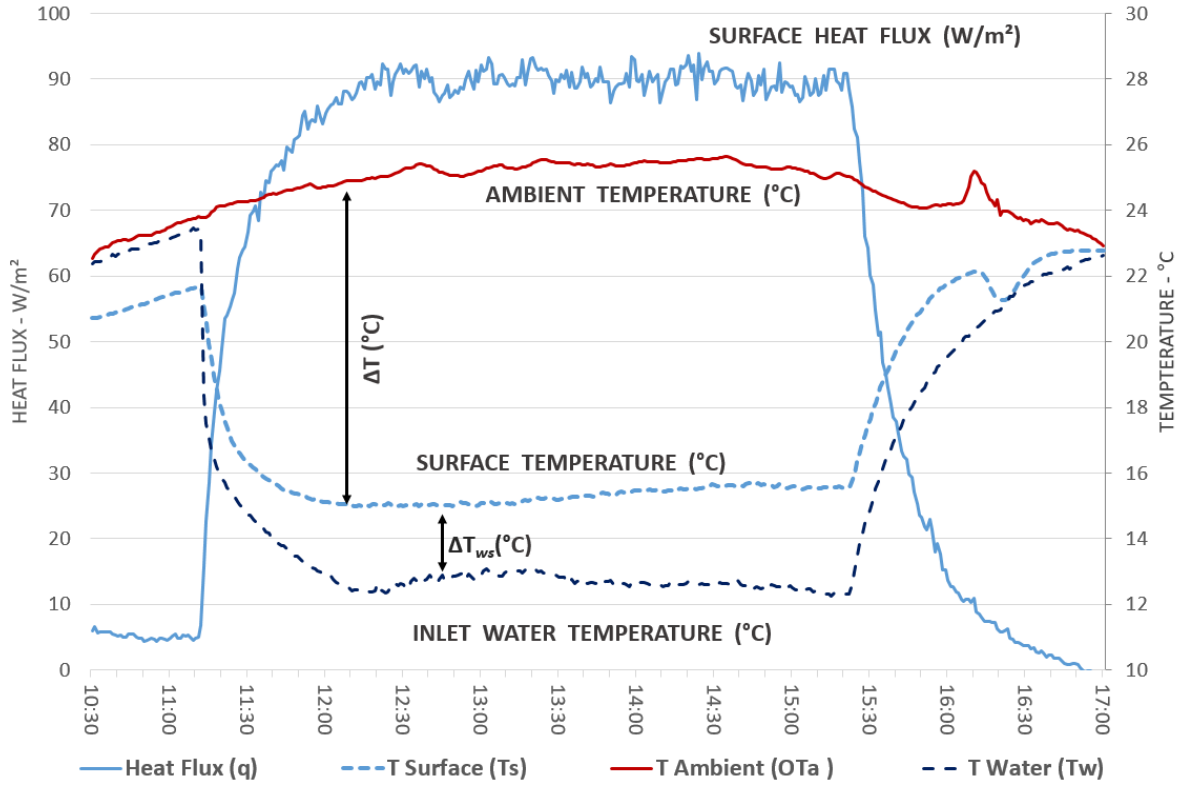

Fig. 3. Measurement and data analysis

The heat transfer between the panels and the conditioned space is the result of the temperature difference between the surface and the operative temperature of the conditioned space (ΔT). The equation below indicates the relationship between heat flux and temperature difference between the radiant surface and the conditioned room [3].

$$q = h_t(OT_a - T_S) \quad \text{(Eq.1)}$$

Where:

q is the total heat flux (W/m²)

h_t is the total heat transfer coefficient (W/m²K)

OT_a is the ambient operative temperature (°C or K)

T_s is the radiant surface temperature (°C or K)

Meanwhile, the normal operation of radiant conditioning systems (without additional latent heat transfer) is represented by the total heat transfer coefficient being the sum of radiant and convective heat transfer coefficients:

$$h_t = h_c + h_r \quad \text{(Eq.2)}$$

Where:

h_c is the convective heat transfer coefficient (W/m²K)

h_r is the radiant heat transfer coefficient (W/m²K)

It is assumed that for most of the heat transfer between the water and the panel's radiant structure, the thermal transmittance (U-value) represents the heat transfer efficiency between the water and the radiant surface and can be calculated based on the formula below.

$$q = (T_s - T_w)U_t \quad \text{(Eq.3)}$$

Where:

U_t is the total U-value (Thermal transmittance) of the panel material structure (W/m²K)

T_s is the temperature of the radiant surface (°C or K)

T_w is the average of the water temperature inside the panel (°C or K)

q is the total heat flux (W/m²)

In this study, auxiliary test runs show that the fast flow rates of the water result in negligible differences between the temperatures of the inlet and outlet water. Hence, the average water temperature can be considered similar to the inlet water temperature.

Combining Eq.1 and Eq.3, it can be concluded that the total heat flux q, or the energy output of a panel, as well as the U-value of a panel, is represented by the temperature difference between the radiant surface and the water inside the panels (ΔT_{ws}). In well-designed panels, the heat transfer between the water and the radiant surface should be efficient; hence, we want minimum temperature differences between the water and the radiant surface. This means that the cooling inlet water temperature can be increased while still achieving the same surface temperature and heat flux, thus reducing the cooling load on the system. This was also the goal of Xing and Li [8] when they proposed a new piping design for a radiant cooling ceiling. They successfully achieve the same heat flux output while increasing the inlet water temperature by 4°C.

In Fig. 3, before the test is commenced, the radiant surface temperature (T_s), water temperature inside the panel (T_w), and ambient operative temperature (OT_a) are relatively close to each other. However, due to the facility's conditions in which the experiments are conducted, the starting radiant surface temperature is slightly lower (1.5°C) than the ambient. As the test commenced, a fixed flow rate (f) of about 13 liters/minute of cooled water entered the manifold of the hydronic mat. In the case of Fig. 3, the water temperature (T_w) is about 12.5°C. The conditioning begins almost immediately when the initial stagnant water in the hydronic mat is replaced. The cooling ceiling operation is evidenced by the heat flux (q) dramatically changing at about 11:15, moving from 5 W/m2 to about 90W/m2 within a few minutes. Such heat transfer results from temperature differences between the radiant surface and the ambient (ΔT); hence, the panel's surface temperature (T_s) is reduced accordingly.

At about 12:15, an equilibrium of the system was reached for the supplied water temperature (T_w) and the ambient environment. Several observations of the panel heat transfer system can be determined from this point onward. First, the temperature difference between the panel's ambient and the surface temperature (ΔT) is to be noted, fixed at approximately 10°C. This temperature difference results in the heat flux (q) of about 90 W/m². Applying equation 1 (Eq.1) to both readings resulted in a total heat transfer coefficient (h_t) of about 9 W/m²K, aligning with the result of our previous study [6] as well as

several other publications [9]. Regarding equation 2 (Eq.2), this total heat transfer coefficient is the sum of radiant and convective heat transfer coefficients [3].

A second point of interest is the difference between the supply water and panel surface temperature (ΔT_{ws}). Again, due to the high flow rate, the average water temperatures can be considered similar to the inlet water temperature. Applying equation 2 (Eq.2), this temperature difference (ΔT_{ws}) represents the heat transfer within the radiant panel material and structure. This is an important phenomenon generally glossed over by panel system manufacturers' specifications. The hydronic mat tubing is embedded into a 10mm plasterboard sheet in this design. The panel yields a 4-5°C temperature difference between the water inlet temperature and the finished surface (ΔT_{ws}). We acknowledge that the finished surface temperature (*Ts*) is critical to producing an increased heat transfer (*q*) between the panel and the ambient environment. However, the finishing material is also a restriction in maximizing heat transfer (*q*). The aim is for this temperature difference between the water supplied and the finishing surface (ΔT_{ws}) to be minimum for the greatest heat transfer effectiveness (*q*).

3.4. Time Constant

In the studies of Yu and Yao [10], Ning et al. [11], and Do et al. [6], the time constant (TC) is used to evaluate how fast the panels react to changes or commands. The time constant can be calculated using Eq.4:

$$y = (initial\ value - final\ value) * e^{-t/TC} + final\ value \quad \text{(Eq.4)}$$

Where:

TC is the time constant (minute)

t is the time between changes (minute)

The time constant (*TC*) is crucial in assessing panel performance. In panel design, thermal connection, and thermal mass can significantly affect the time constant [6]. Additionally, the panels' commencing

and ceasing time constants will be examined. The commencing time constant represents the reaction time of the panel when the system is started, and cold water is supplied to the panel. Meanwhile, the ceasing time constant represents the "cool down" periods as the system is shut down when the cold water supply is cut off and the radiant surface temperature returns to near ambient temperature.

3.5. Data Analysis

To evaluate the designs, the performances of the prototype panels are compared relatively with each other. This approach is also the preferred method of analyzing and evaluating new radiant panel designs, as demonstrated in the research of Xing and Li [8] or Yin et al. [12]. The parameters considered in the comparisons are the total heat flux (q), the temperature difference between inlet water and the radiant surface (ΔT_{ws}), and the time constant (TC).

The panels are examined in three groups of four. In each comparison, the better design would yield higher heat flux (q) with a lower difference between inlet water temperature and surface temperature (ΔT_{ws}) and a lower time constant (TC). The inlet water temperature is the same in each test, so a higher heat flux (q) indicates higher capacity. At the same time, a lower ΔT_{ws} means higher thermal transmittance (U-value) and, therefore, a better panel design. Also, the lower time constant shows a panel design with a lower reaction time. The result of the panel performance will be investigated to find the pros and cons of the panel design and construction method. The lessons learned from the tests will be used to improve the panel design.

4. Instrumental Experiment

4.1. Equipment and sensors

As shown in Table 1, the required data is collected with four types of equipment: heat flux sensors, a thermal comfort cart, a thermal imaging camera (Fig. 4), and thermal couples. The heat flux sensors are FHF05 foil sensors, supplied pre-calibrated and certified. Four were used to collect the heat flux data in each test.

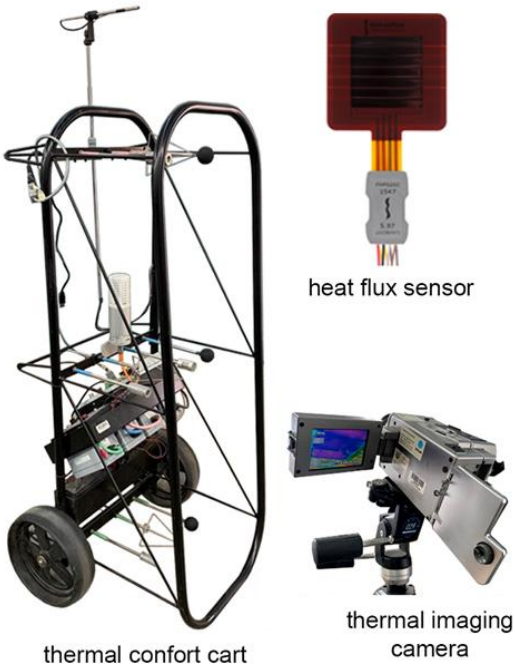

Fig. 4. Experimental Instrument

To ensure accurate readings, in preliminary test runs, the heat flux sensors are cross-checked against each other. A Dobros Precision mercury thermometer is calibrated for the thermocouples for less than 0.5°C error. An AVIO Neo Thermo TVS-700, thermal imaging camera assists the heat flux sensors and thermocouples. Campbell Scientific CR10X Logger Boards collect readings from the heat flux sensor and the thermocouples.

The thermal comfort cart used is an ASHRAE-compliant field study instrument, as used by De Dear and Brager [13] or Luther et al. [14]. This instrument consists of sensors, including a thermistor, air velocity, humidity, black globe temperature sensors, and a CO_2 meter. It is capable of measuring elements needed to calculate the operative temperature. A Campbell Scientific CR23X Datalogger is used to collect the readings from the sensors of the comfort cart. Finally, a digital flow meter is used to monitor the flow rate of the inlet water.

4.2. Experiment Setup

The experimental setup is shown in Fig. 5. Panels, in groups of four, are connected to a single radiant ceiling system located within an industrial shed. Table 2 shows the panel and their location in each test. The ceiling is 3m high above the floor. The experiments are conducted in a large metal shed which can protect the experiments from the external environment while emulating an open office space.

Table 2

Experiment test runs and associated panels.

	Position	Position 2	Position 3	Position 4
Test 1	Design 1 (P1)	Design 2 (P2)	Design 3 (P3)	Design 4 (P4)
Test 2	Design 1 (P1)	Design 2 (P2)	Design 3 (P3)	Design 5 (P5)
Test 3	Design 1 (P1)	Design 2 (P2)	Design 3 (P3)	Design 6 (P6)

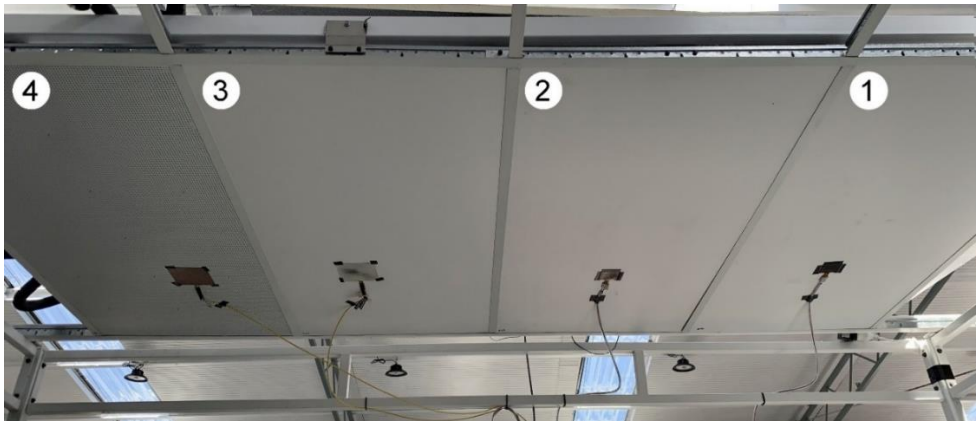

Fig. 5. Ceiling test panel experimental setup

The radiant ceiling system also includes a hydronic control panel and an air-to-water heat pump that provides cold water. The hydronic control panel consisting of valves, a pump, a flow sensor, and a pressure vessel pumps cold water from the heat pump to the radiant panel. Equal flow paths of the water through all of the panels are required; hence, the "canopy to canopy" arrangement is utilized to ensure equal water distribution to all four radiant panels,

A heat flux sensor is installed at the center area of each panel to monitor the heat exchange between the panel and the environment (q). The locations of the heat flux sensors are chosen with the aid of the

thermal imaging camera in a preliminary test run. The resulting thermograph shows that the surface temperature at the center of the panel is relatively uniform and more representative of the panel operation than the edge area (Fig. 6). This arrangement is similar to the experiment setup of Gallardo and Berardi [15] and Li, Yoshidomi [16]. Four thermocouples are used to measure the water temperature at the inlet point of each panel.

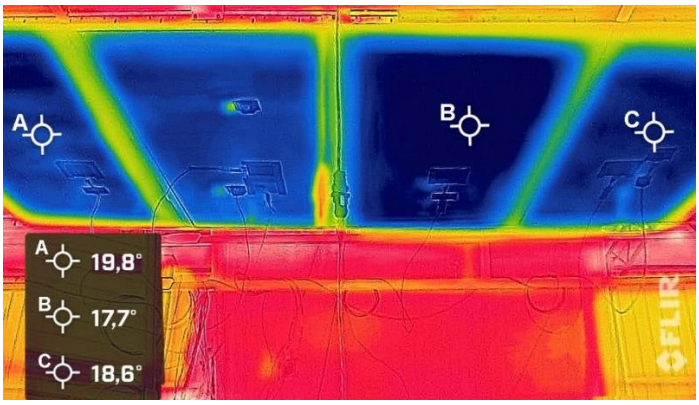

Fig. 6. Thermographic image of the test panels in experiment mode

4.3. Experiment Principle

The experiments are conducted to examine the performance of radiant cooling ceiling panels. Hence, hot sunny days with air temperatures above 26°C are chosen to run the experiment. Between 10 am and 5 pm on such days, the operative temperature at the site of the experiment can be upward of 30°C and is therefore highly suited for running cooling operations. In Test 1, the heat pump and the radiant system are activated simultaneously, while in Tests 2 and 3, the cold water is prepared before the test runs.

Cold water is pumped and circulated through the panels as the experiments commence. The system is operated at full capacity, and the water flow rate is about 13 liters/minute. During the test runs, the heat pump is kept running. A test run lasts about three hours, and as the test run concludes, the whole system, including the heat pump, the pump, and the vales, is shut down, and the panels are isolated from any cooling sources. The panels will then be left to "cool down" independently. The measuring equipment is activated about half an hour before each test run. It continues to monitor for at least one hour after the system is shut down, thus recording the data before, during, and after the operation.

5. Experiment Results

This section presents the results of the three official test runs and provides preliminary discussions.

5.1. Test 1

At the outset, as the system turned on and the cold water was supplied to the panels, the inlet water temperature (T_w) instantly dropped from 30 to 19°C. In the next hour, as the heat pump continued to run, the inlet water temperature (T_w) decreased from 19°C to 15°C and was stable. This drop in water temperature (T_w) is the result of the heat pump running and indicates that the heat pump operation affects the panel's performance, especially in terms of time constant.

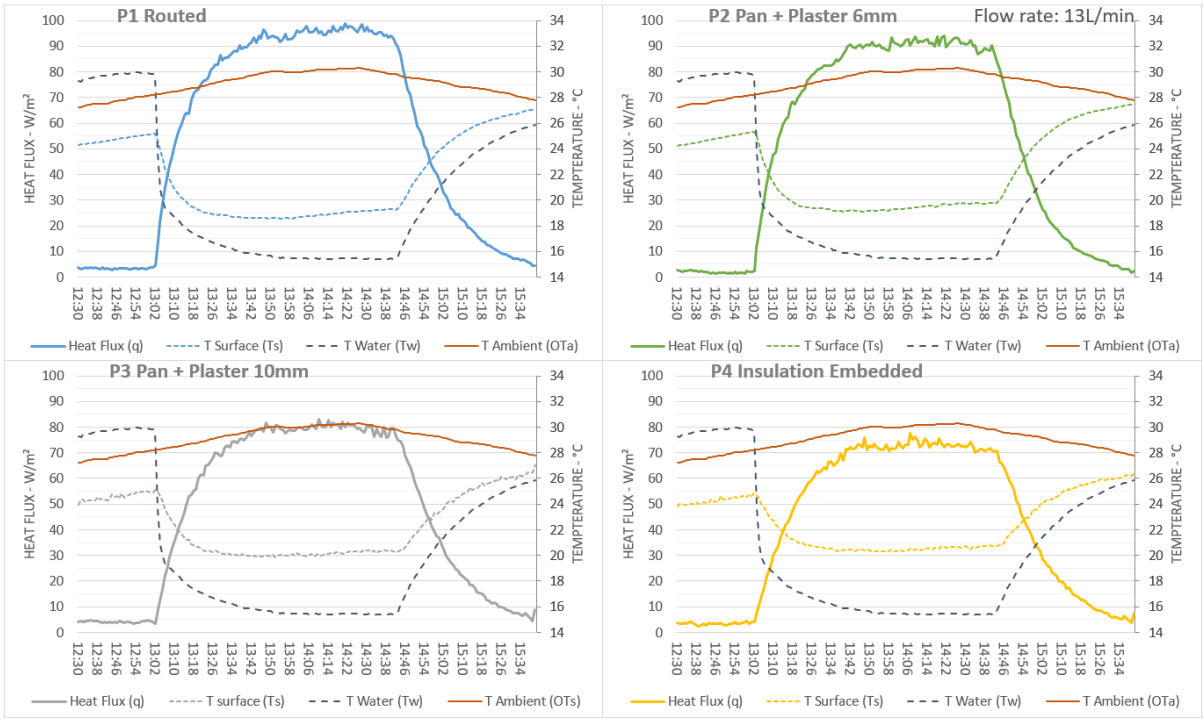

Fig. 7. Test Run 1: Charted Results for four Panels

Interestingly, at the beginning of the test run, all the panels' surfaces (T_s) are about 25°C, 3°C lower than the ambient. Meanwhile, the inlet temperature (T_w) reading is 2°C higher than the ambient. However, at the end of this test run, when the system is cooled down, the operative ambient temperature (OT_a), the surfaces' temperatures (T_s), and the water temperature (T_w) reverted close to each other. Considering that the sensors are rigorously calibrated, and the readings of different sensors at four

different panels are consistent, it can be concluded that these are the conditions in the experiment area at that time, and the sensors perform correctly. However, it must be noted that the metal shed in which the experiments were conducted only provided limited protection to the experiment against the rapid change of weather conditions in Victoria, Australia.

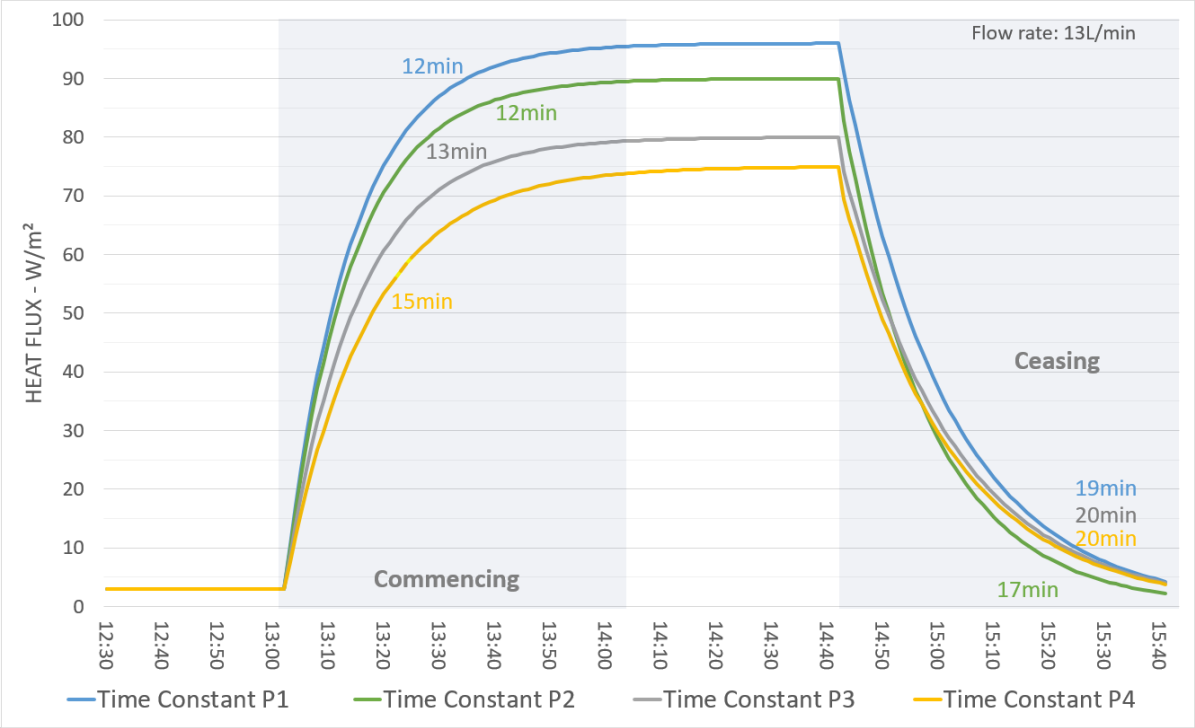

Fig. 8. Test 1 Time constant

Regarding heat flux (q), the panel of Design 1 (P1 Routed) yields the best result reaching about 95W/m². The heat flux reading for the panel of Design 2 (P2 Pan + Plaster 6mm) follows closely and peaks at about 90W/m². Meanwhile, the heat flux (q) reading for Design 3 (P3 Pan + Plaster 10mm) can only reach 80W/m² and it is 75W/m² for Design 4 (P4 Insulation Embedded). The order of the heat flux readings is confirmed by the surface temperatures (T_s). Design 1 reaches the lowest cooling surface temperature (T_s) at about 18.5°C. Meanwhile, the surface temperature (T_s) of Design 2 (P2 Pan + Plaster 6mm) reaches 19 °C, and it is 20°C and 20.5°C for Design 3 (P3 Pan + Plaster 10mm) and 4 (P4 Insulation Embedded) respectively. Equation 1 (**Eq.1**) allows the total heat transfer coefficient (h_t) to be calculated. The result transfer coefficient (h_t) should be the same as the panels are tested in the same

condition. As predicted, the four panels' peak transfer coefficient (h_t) calculated heat values are the same at about 8 W/m²K.

Fig. 8 shows the time-constant result of this test run. For the commencing time constant, panels of Design 1, 2, and 3 (P1, P2, and P3) yield similar results at about 12-13 minutes, while the panel of Design 4 (P4) has the longest commencing time constant of 15 minutes. Of note, the commencing time constant is different from the ceasing time constant. The ceasing time constant of the panels of Design 1, 3, and 4 (P1, P3, and P4) are close to each other at about 19-20 minutes. However, the panel of Design 2 (P2) yields a shorter time constant of 17 minutes. Table 3 summarizes the results of test run 1.

Table 3

Summary of results for test run 1

TEST 1	q (W/m²)	T_s (°C)	ΔT (°C)	ΔT_{ws} (°C)	h_t (W/m²K)	Commencing TC (minutes)	Ceasing TC (minutes)
Design 1 (P1)	95	18.5	11.5	3	8.2	12	19
Design 2 (P2)	90	19	11	3.5	8.2	12	17
Design 3 (P3)	80	20	10	4.5	8	13	20
Design 4 (P4)	75	20.5	9.5	5	7.9	15	20

5.2. Test 2

Fig. 9 shows the panel performance results of Test 2. This test examines panels of Design 1, 2, 3, and 5 (P1, P2, P3, and P5). At the outset, the surface temperature of the four panels (T_s), the ambient air temperature, and the inlet water temperature (T_w) are relatively close to each other at about 32°C, indicating a stable and uniform condition at the testing site. The ambient temperature (OT_a) steadily rose to about 37°C. The inlet water temperature (T_w) is about 11°C, and the flow rate is about 13L/minute.

Due to the high-temperature difference between the inlet water and the ambient environment, high heat flux was expected. The heat flux (q) reading of Design 1 (P1 Routed) peaked at about 190 W/m². Panels of Design 2 (P2 Pan + Plaster 6mm) and 3 (P3 Pan + Plaster 10mm) also yielded high heat flux (q) readings that peak at about 170 W/m². Remarkably, the exposed panel of Design 5 (P5 Exposed) yields an exceptionally high heat flux (q) reading reaching 280W/m2.

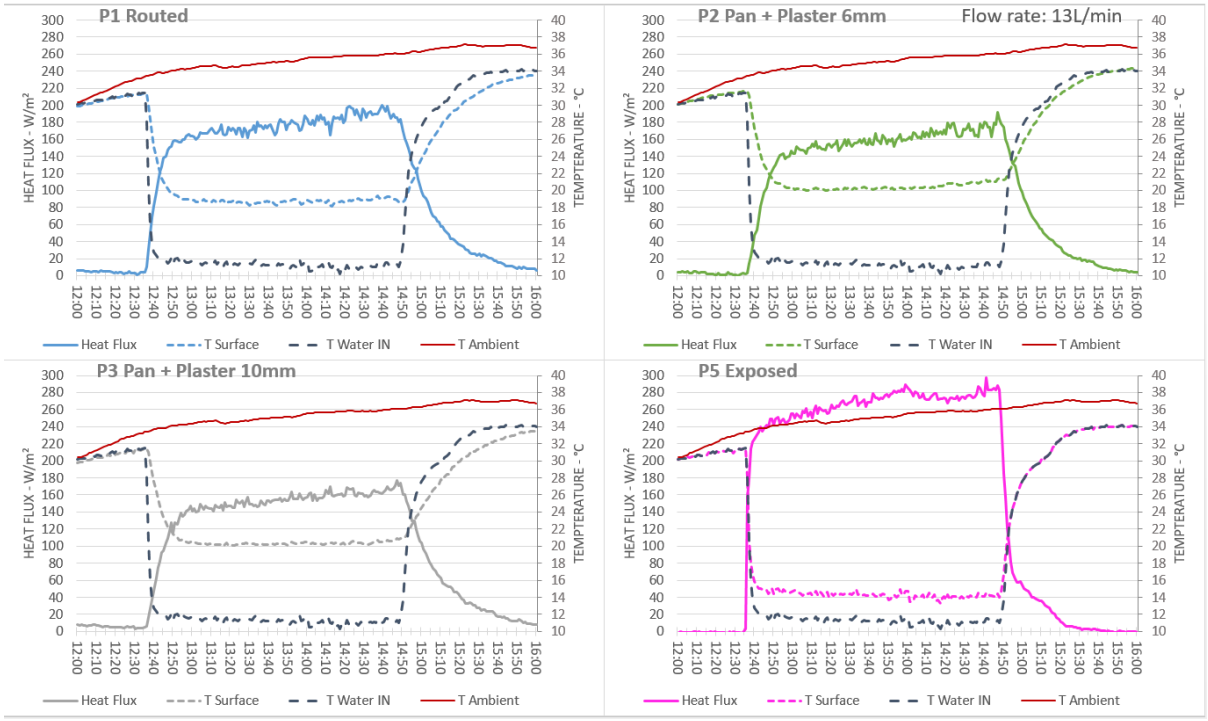

Fig. 9. Test 2 Panels' performance

It may be interesting to realize that the exposed panel results yield the ultimate cooling potential possible for the material composition in our hydronic panel design. Since this exposed panel has no finishing substrate, it demonstrates the highest possible heat transfer or cooling potential. Such high thermal performance is one of the most revealing aspects of our experimental study and will undoubtedly influence newer panel designs as we seek to get the most heat transfer out of a panel.

The surface temperature readings (T_s) also reflect the heat flux readings above. It is realized that Designs 1, 2, and 3 (P1, P2, and P3) all have similar surface temperatures (T_s) at about 19 to 20 °C. The results indicate a total heat transfer coefficient of about 11W/m²K (h_t) for these three panels. This total heat transfer coefficient (h_t) is much higher than the 8 W/m²K result of Test 1 and even the 10 W/m²K coefficient value of our previous study [6] but matches the value reported in the RHEVA handbook [3]. Notably, the Design 5 panel (P5 Exposed) stands out, with a surface temperature (T_s) 4 °C lower than Design 1, reaching 15°C. However, applying this result and the heat flux (q) reading of 280 W/m² to Eq.1 registers a staggering heat transfer coefficient (h_t) of 13.3W/m²K.

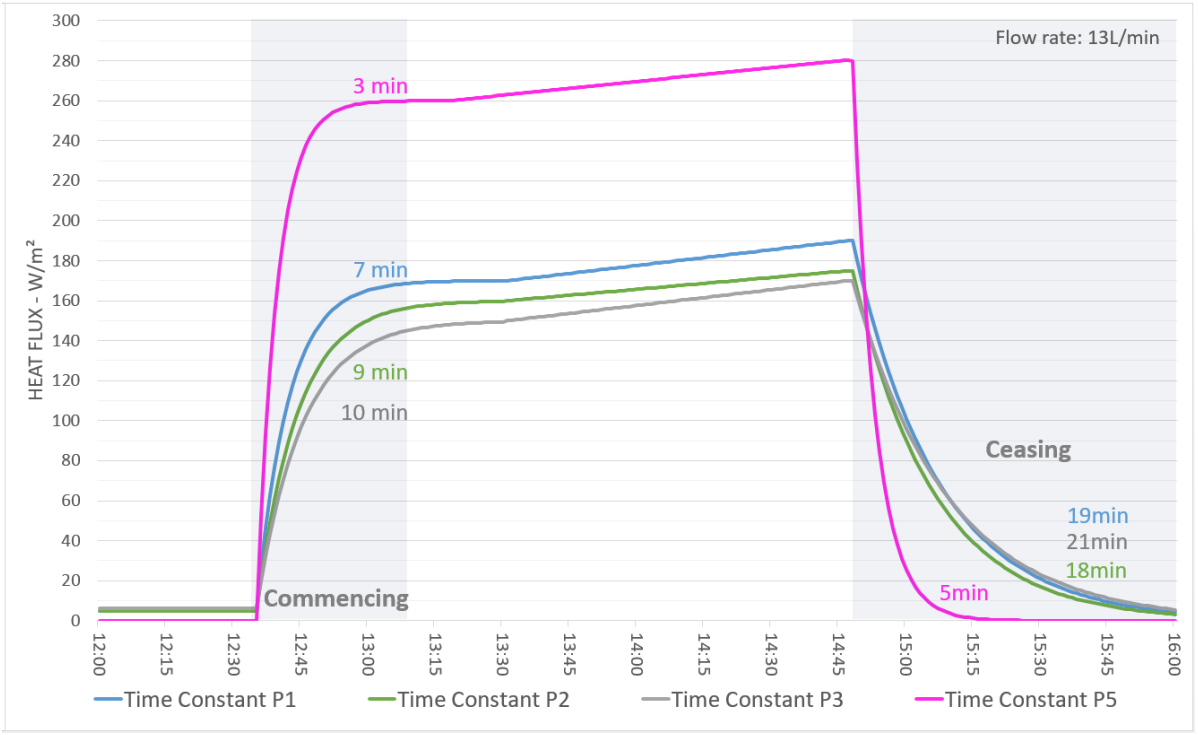

Fig. 10. Test 2 time constant

Regarding the commencing time constant in this test, the result for Design 5 (P5 Exposed) is only 3 minutes, while it is 7 minutes for Design 1 (P1 Routed), 9 minutes for Design 2 (P2 Pan + Plaster 6mm), and 10 minutes for Design 3 (P3 Pan + Plaster 10 mm). Also, the ceasing time constant of Design 5 (P5 Exposed) is only 5 minutes, which is significantly lower than the ceasing time constant of 20 minutes of the other three. Table 5 below summarizes the results of test run 2.

Table 5

Summary of test run 2 results.

TEST 2	q (W/m²)	T_s (°C)	ΔT (°C)	ΔT_{ws} (°C)	h_t (W/m²K)	Commencing TC (minutes)	Ceasing TC (minutes)
Design 1 (P1)	190	19	17	19	11.2	7	19
Design 2 (P2)	175	20	16	29	10.9	9	18
Design 3 (P3)	170	20	16	19	10.7	10	21
Design 5 (P5)	280	15	21	4	13.3	3	5

5.3. Test 3

Fig. 11 shows the panel performance results of Test 3, which involves panels of Design 1, 2, 3, and 6 (P1, P2, P3, and P6). Before the test is started, the conditions are similar to that of Test 1. The inlet water temperature (T_w) is close to the ambient temperature (OT_a) at about 32°C. However, the panels' surface temperatures (T_s) are only about 29°C. This can be attributed to the rapid weather change and the water temperature in each panel at the start of each experiment. This test's inlet water temperature (T_w) is about 15°C, and the flow rate is about 13L/minute.

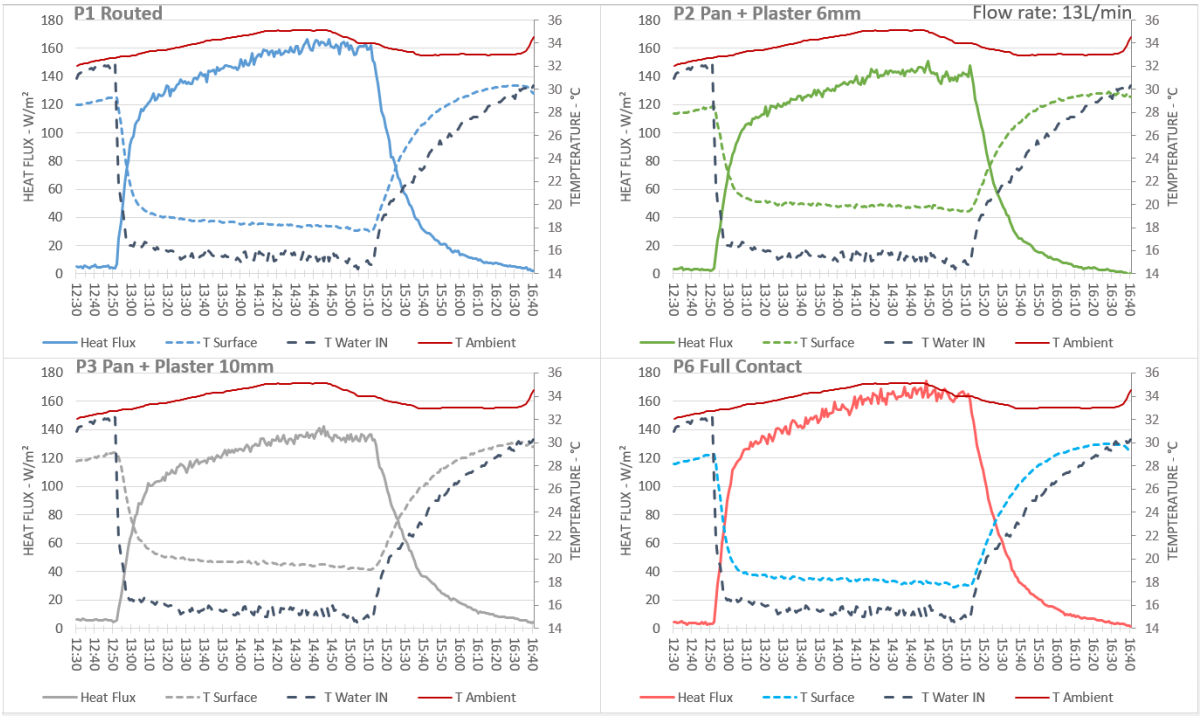

Fig. 11. Test 3 Panel's performance

In terms of energy output, panels of Designs 1 (P1 routed) and 6 (P6 Full Contact) yield similar heat flux readings (q). The readings peak at about 160W/m² for Design 1 (P1 routed) and 165W/m² for Design 6 (P6 Full Contact). Meanwhile, the panel of Design 2 (P2 Pan + Plaster 6mm) only yields about 135 W/m² and is closely followed by Design 3 (P3 Pan + Plaster 10mm) with 130 W/m². The heat flux (q) readings are reflected by the panels' surface temperature (T_s). Panels of Design 1 (P1 routed) and 6 (P6 Full Contact) have similar surface temperatures (T_s) at about 18°C while it is about 19°C to 20°C for panels of Design 2 (P2 Pan + Plaster 6mm) and 3 (P2 Pan + Plaster 6mm). Applying Eq.1 to the

readings results in a total heat transfer coefficient (ht) of about 9 W/m²K for all four panels. This heat transfer coefficient (h_t) value is within the range of 8 to 10W/m²K of earlier studies [9]. Also, the similar coefficient results from the 4 different panels validate the readings of the sensors.

For the Commencing time constant of this test, Design 6 (P6 Full Contact) has the best result at 7 minutes, followed closely by Design 1 (P1 Routed) at 8 minutes. Panels of Design 2 (P2 Pan + Plaster 6mm) and 3 (P3 Pan + Plaster 10mm) have a similar commencing time constant of 9 minutes. Interestingly, the panels of Design 1, 2, and 6 (P1, P2, and P6) have the same ceasing time constant of 18 minutes, while the Design 3 (P3 Pan + Plaster 10mm) panel has a higher result of 23 minutes. The results of Test 3 are summarized in Table 6. below.

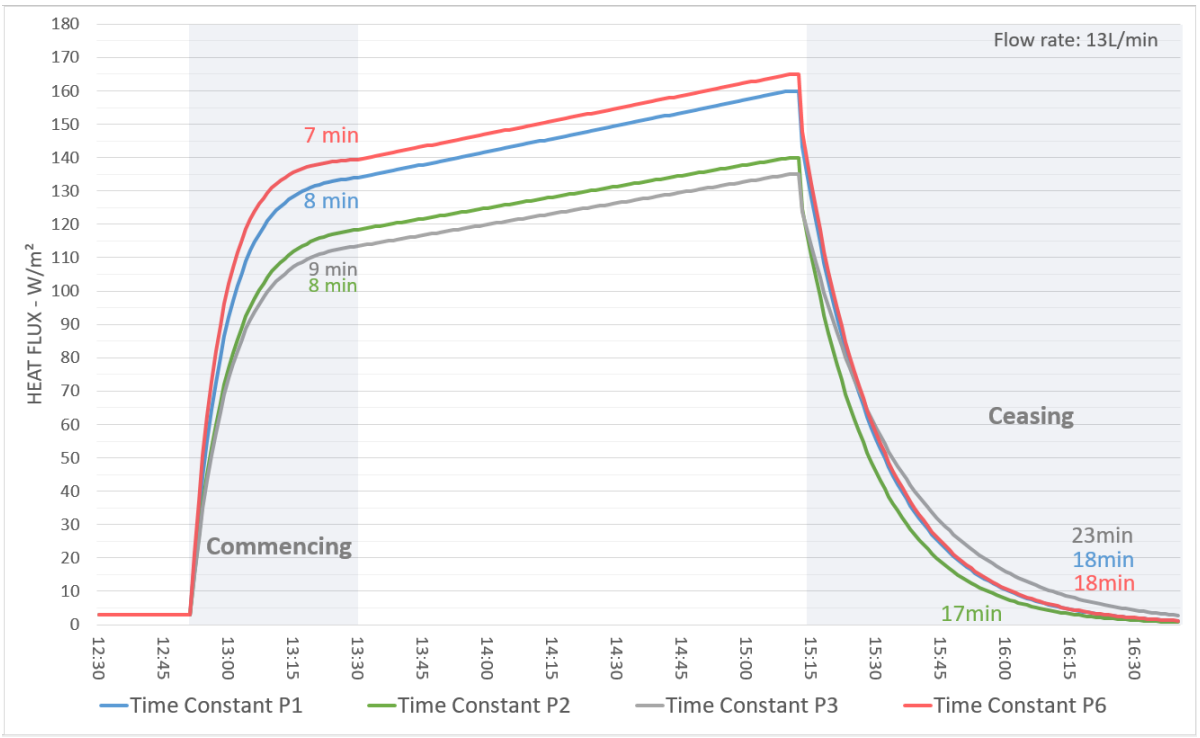

Fig. 12. Test 3 time constant

Table 6

Summary of test run 3 results.

TEST 3	q (W/m²)	T_s (°C)	ΔT (°C)	ΔT_{ws} (°C)	h_t (W/m²K)	Commencing TC (minutes)	Ceasing TC (minutes)
Design 1 (P1)	160	18	16	3.5	8.9	8	18
Design 2 (P2)	135	19	14	4.5	9.3	8	17
Design 3 (P3)	130	20	15	5	9	9	23
Design 6 (P6)	165	18	16	3	9.1	7	18

6. Discussion

6.1. Test 1 – Heat Transfer

Test run 1 confirms the effect of thermal connection on the heat transfer and the capacity of the panels. Embedding the capillary tubes in the radiant surface, like in Design 1 (P1 Routed), proved the most effective design. Such effectiveness is the reason why Design 1 is the industry's common standard construction used presently by suppliers, even though this design proves to be quite taxing. In contrast, having a metal pan to aid in heat transfer also proves to have a positive effect, notably increasing the heat transfer capacity of the cooling panels, especially when comparing the performance of Design 2 (P2 Pan + Plaster 6mm) and 4 (P4 Insulation Embedded).

The panels of these two designs are similar, using the same gypsum ceiling tile board, and only differ in the metal pan used in Design 2. Yet, the panel of Design 2 (P2 Pan + Plaster 6mm) yields about 15W/m² higher and has a lower commencing time constant. In terms of design knowledge, the metal pan used in the panels of Designs 2 (P2 Pan + Plaster 6mm) and 3 (P3 Pan + Plaster 10mm) can be seen as an effective design, behaving as a thermal connection or a heat-conducting element between the capillary tube and the radiant surface. This also confirms the recommendation of the RHEVA handbook for type B embedded systems (ESS), which states that such a “heat-conducting element” is required [3].

6.2. Test 2 – Thermal Mass and Therma Resistance

This test is conducted to investigate further the effect of thermal resistance and thermal mass on panel performance. Hence, the main focus is to evaluate the Design 5 (P5 Exposed) panel, which has no extra radiant surface resistance or thermal mass compared to other panels. The results show significant

differences in performance between the Design 5 panel (P5 Exposed) and other panels in terms of heat flux (q), surface temperature (T_s), and time constant (TC). While panels of Design 1, 2, and 3 (P1, P2, and P3) have their heat flux output (q), surface temperatures, and time constants relatively close to each other, those of Design 5-panel (P5 Exposed) stand out with about 50% more heat flux (q), at least 4°C lower surface temperature (T_s) and the time constants (TC) can be 3 times lower. Such results also prove the significant impact of thermal resistance and thermal mass on cooling panels' capacity and reaction times. Although Design 5 (P5 Exposed) may not be viable in realistic projects due to the lack of a finishing layer and architectural appeal, its exceptionally high heat flux output and low response times demonstrate the radiant cooling panel's full potential.

The thermal resistance between the water and the radiant surface must be reduced to increase the cooling panel capacity. Such improvement will also reduce the temperature difference between the radiant surface and the inlet water temperature (ΔT_{ws}). In turn, lower ΔT_{ws} means in achieving the desired cooling surface temperature (T_s) and heat flux output (q), the inlet water temperature (T_s) can be higher, reducing the load on the heat pump and making the whole radiant cooling system more energy efficient.

6.3. Test 3 – Full Contact

The most important result of test 3 is confirming the effectiveness of Design 6 (P6 Full Contact). Design 6 (P6 Full Contact) is a type B embedded system (ESS) that closely follows the recommendations of the RHEVA handbook [3]. In particular, the design includes "heat-conducting elements" to evenly distribute heat and provides an improved thermal connection between the water capillary tubes and the radiant surface. However, implementing such design elements is not clearly emphasized in the RHEVA handbook.

In Design 6 (P6 Full Contact), the metal pan is the "heat-conducting element" while the adhesive provides a much-needed thermal connection enhancement. The metal pan is an effective heat-conducting element, as shown in Test 1. In Test 3, the full contact adhesion method enhances the

thermal conductivity between the water tubes, the metal pan, and the radiant surface. The effect of the adhesion method is evident when comparing Design 2 (P2 Pan + Plaster 6mm) and 6 (P6 Full Contact). The two designs are almost identical and have similar weights; the only difference is the attention given to a full contact adhesion in Design 6 (P6 Full Contact). Yet, in Test 3, the panel of Design 6 (P6 Full Contact) yielded about 22% more heat flux and a faster commencing time constant.

The result proves that Design 6 is highly effective, and its performance rivals that of Design 1 (P1 Routed). In addition, the prototyping construction process of Design 6 (P6 Full Contact) faced no significant difficulties. The panel is built with relative ease. Even the adhesive used in the panel is not specialized but is commonly used and widely available on the market. A specialized thermal conducting adhesive may be explored and tested in further developments.

6.4. Heat Transfer Coefficient and Condensation

Throughout the three tests, the calculated heat transfer coefficient (h_t) values range mostly between 8 to 11 W/m²K. Such a range of values matches the recorded heat transfer coefficient documented in previous review publications [9]. In particular, the resultant heat transfer coefficient (h_t) of Test 1 is about 8 W/m²K and 9 W/m²K for Test 3. However, in Test 2, three panels indicated heat transfer coefficient (ht) values of around 11 W/m²K. In the panel Design 5 (P5 Exposed), this was a staggering 13.3 W/m²K. Although the heat transfer coefficient (h_t) value of 11 W/m²K is recommended in the RHEVA Handbook [3] it is not often achieved in experiments conducted in previous studies [9]. Meanwhile, the heat transfer coefficient (h_t) of 13.3 W/m²K highly warrants further discussion.

Applying equation 2 (Eq.2), in normal operation, the total heat transfer coefficient (h_t) in radiant cooling consists of radiant and convective heat transfer coefficients [3]. The radiant heat transfer coefficient (h_r) is generally agreed among researchers to be fixed at 5.5 W/m²K [9]. Hence, to increase the total heat flux (q) and heat transfer coefficient (h_t), the convective heat transfer should be improved, with the preferred method being increasing air velocity. For example, in the research conducted by [17] or [5] the cooling capacity of radiant ceiling panels can be notably enhanced by promoting air movement.

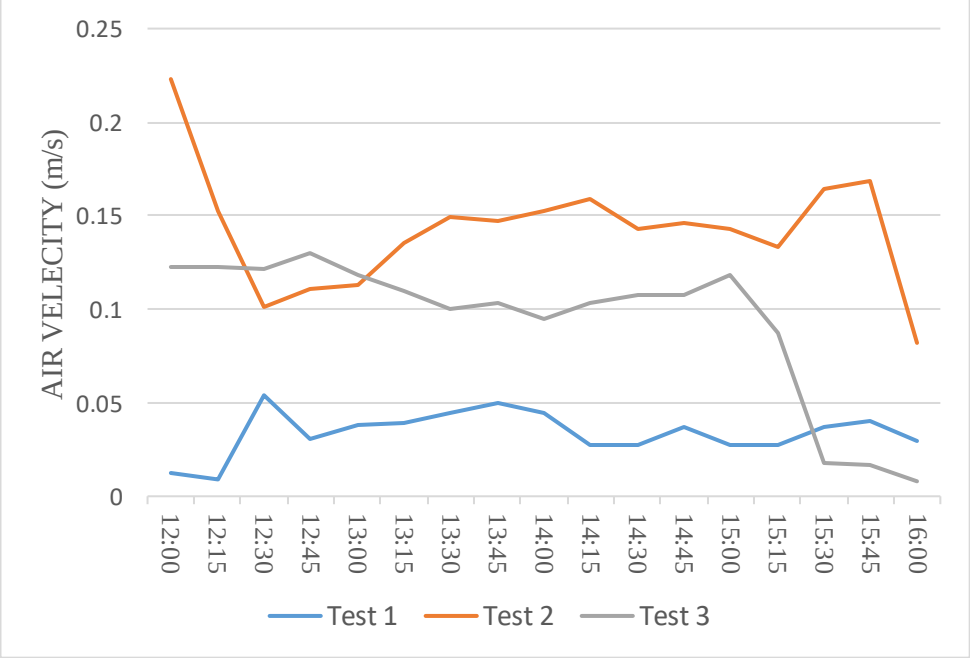

Fig. 13. Air velocity in all three tests

The study of Chiang, Wang [18] even concludes that radiant cooling ceiling systems may not be able to provide thermal comfort without convection aid. Hence, the heat transfer coefficient (h_t) value of 11 W/m²K in test 2 is most likely the result of high air velocity near the radiant surface. Fig. 13 shows the thermal comfort cart's air velocity (v) recorded. Comparing the air velocity (v) readings with the heat transfer coefficient (h_t) results of the three tests, there is evidence showing that higher air velocity (v) could lead to a higher total heat transfer coefficient (h_t). Yet, in all of the tests, the panels are located next to each other, which should result in a similar total heat transfer and convective heat transfer coefficient.

Further examination shows that in Test 2, the surface temperature (T_s) of the Design 5 (P5 Exposed) panel is 14 °C, which is lower than the 16°C recommended by the RHEVA handbook to prevent condensation [3]. As condensation did take place on the radiant surface of the Design 5 (P5 Exposed) panel in Test 2 (Fig. 14), it can be concluded that the latent heat transfer and condensation have notable contributions to the exceptionally high heat flux and heat transfer coefficient in this case. If such additional heat transfer can be utilized, the capacity of radiant cooling panels could be significantly

improved. A similar approach is even suggested by Zhong et al. [19]. The authors use superhydrophobic material as the radiant surface of cooling panels to prevent droplets from forming. This radiant surface design allows cooling panels to operate below the dewpoint and take advantage of latent heat transfer, thus significantly enhancing cooling capacity.

Fig. 14. Condensation on the 'exposed' panel of Design 5

6.5. Time Constant

As Panels of Design 1, 2, and 3 (P1, P2, and P3) are involved in all three tests, it is possible to compare the time constants of the three panels. The commencing time constants of Design 1, 2, and 3 in Test 1 are from 12 to 13 minutes, notably higher than that of Test 2 and 3 at 7 to 10 minutes. In this case, the heat pump operation seems to have significant effects on the commencing time constant. In tests 2 and 3 however, the commencing time constants of the three panels are relatively stable.

The ceasing time constants of the three panels are also quite stable throughout the tests. For Design 1 (P1 Routed), the time constant is 19, 18, and 18 minutes from Test 1 to Test 3, respectively. As for Design 2 (P2 Pan + Plaster 6mm) is 17 minutes in Test 1, 18 minutes in Test 2, and 17 minutes in Test 3. The time constant of Design 3 (P3 Pan + Plaster 10mm) is also stable, with 20 minutes in Test 1, 21 minutes in Test 2, and 23 minutes in Test 3. It is worth noting that the panel with a lower weight has a lower time constant in all of the tests. In particular, the Design 2 panel (P2) is the lightest and has the

lowest ceasing time constants, while the time constants of the heaviest Design 3 panel (P3) are the highest. This stability and consistency validate the tests and confirm that the ceasing time constant of a radiant panel may not be affected by operation conditions such as water temperature, flow rate, or operative temperature but mainly result from the panel's thermal mass [6]. The gypsum tiles (radiant surface) of the panels in this study account for most of the thermal mass.

7. Conclusion

In conclusion, this study examines the performance of six different designs for radiant cooling ceiling panels. Three tests are conducted, and several conclusions can be drawn from the results.

- Design 6 is an effective design for radiant cooling ceiling panels. To achieve high heat flux output and low time constant, this panel design closely follows the recommendation of the RHEVA handbook for Type B embedded systems, with an adequate heat-conducting element (metal pan) and an effective thermal connection (full contact adhesion). This design is also easy to prototype and may be feasible for mass production. In summary, Design 6 (P6 Full Contact) is a practical and effective implementation of such design knowledge.
- Thermal resistance and thermal mass significantly impact radiant cooling panels' performance. Further cooling panel design should focus on minimizing these two parameters to increase the radiant panels' efficiency. Such improvement can make the panel more responsive and reduce energy use across the system.
- Depending on the operating condition, the total heat transfer coefficient of the radiant cooling can vary vastly, from 8 to 11 W/m^2K. A higher convective heat transfer coefficient is required to achieve a higher total heat transfer coefficient.
- When condensation occurs on the radiant panel, latent heat transfer is added to the overall heat transfer process, leading to a notable increase in heat flux and the heat transfer coefficient. If utilized correctly, latent heat transfer can significantly improve the cooling capacity of radiant panels.

The results of this experimental study are highly encouraging. Consequently, we intend to develop and build upon the designs presented in this report further. Also, a test chamber that emulates the design configuration of a perimeter zone for an office in Australia is being built to evaluate radiant conditioning performance in a realistic environment. The reporting of research experiments in this 'test cell' environment is intended for our future work.

DISCLAMER

We confirm that there is no patents attached to this work.

References

1. Rhee, K.-N., B.W. Olesen, and K.W. Kim, *Ten questions about radiant heating and cooling systems.* Building and Environment, 2017. **112**: p. 367-381.
2. Rhee, K.-N. and K.W. Kim, *A 50 year review of basic and applied research in radiant heating and cooling systems for the built environment.* Building and Environment, 2015. **91**: p. 166-190.
3. Babiak, J., B.W. Olesen, and D. Petras, *Low temperature heating and high temperature cooling: REHVA GUIDEBOOK No 7.* 2007.
4. Do, H.Q., et al. *Optimizing conditioning systems in the perimeter zones of office buildings*. in *ASA 2022: Building on knowledge, theory and practice: Proceedings of the 55th Annual Conference of the Architectural Science Association*. 2022. Architectural Science Association.
5. Shin, M.S., et al., *Enhancement of cooling capacity through open-type installation of cooling radiant ceiling panel systems.* Building and Environment, 2019. **148**: p. 417-432.
6. Do, H.Q., et al., *Development and thermal performance testing of radiant conditioning ceiling panels.* Architectural Science Review, 2024: p. 1-12.
7. Mosa, M., M. Labat, and S. Lorente, *Constructal design of flow channels for radiant cooling panels.* International Journal of Thermal Sciences, 2019. **145**: p. 106052.
8. Xing, D. and N. Li, *Reconstruction of hydronic radiant cooling panels: Conceptual design and numerical simulation.* Thermal Science and Engineering Progress, 2022. **30**: p. 101272.
9. Shinoda, J., et al., *A review of the surface heat transfer coefficients of radiant heating and cooling systems.* Building and Environment, 2019. **159**: p. 106156.
10. Yu, G. and Y. Yao, *The experimental research on the heating and cooling performance of light floor radiant panels.* Procedia Engineering, 2015. **121**: p. 1349-1355.
11. Ning, B., S. Schiavon, and F.S. Bauman, *A novel classification scheme for design and control of radiant system based on thermal response time.* Energy and Buildings, 2017. **137**: p. 38-45.
12. Yin, Y., et al., *Experimental investigation on the heat transfer performance and water condensation phenomenon of radiant cooling panels.* Building and environment, 2014. **71**: p. 15-23.
13. De Dear, R. and G.S. Brager, *The adaptive model of thermal comfort and energy conservation in the built environment.* International journal of biometeorology, 2001. **45**(2): p. 100-108.

14. Luther, M., O. Tokede, and C. Liu, *Applying a comfort model to building performance analysis.* Architectural Science Review, 2020. **63**(6): p. 481-493.
15. Gallardo, A. and U. Berardi, *Experimental evaluation of the cooling performance of radiant ceiling panels with thermal energy storage.* Energy and Buildings, 2022. **262**: p. 112021.
16. Li, R., et al., *Field evaluation of performance of radiant heating/cooling ceiling panel system.* Energy and Buildings, 2015. **86**: p. 58-65.
17. Ye, M., et al., *Thermal performance of ceiling radiant cooling panel with a segmented and concave surface: Laboratory analysis.* Applied Thermal Engineering, 2021. **196**: p. 117280.
18. Chiang, W.-H., C.-Y. Wang, and J.-S. Huang, *Evaluation of cooling ceiling and mechanical ventilation systems on thermal comfort using CFD study in an office for subtropical region.* Building and Environment, 2012. **48**: p. 113-127.
19. Zhong, Z., et al., *Enhancing the cooling capacity of radiant ceiling panels by latent heat transfer of superhydrophobic surfaces.* Energy and Buildings, 2022. **263**: p. 112036.